**Supplemental Figure 1, Related to Figures 1, 2 and 3: Experimental Strategy and immunostaining demonstrating loss of Arx and Dnmt1 in knock-out mice**

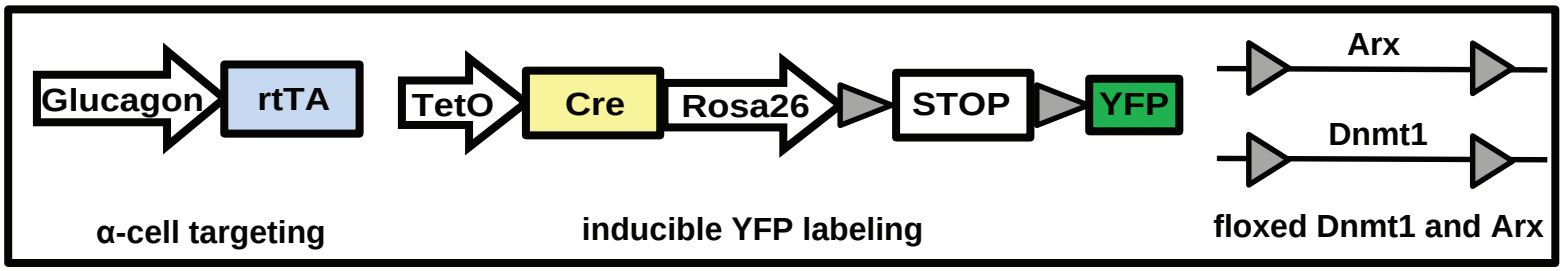


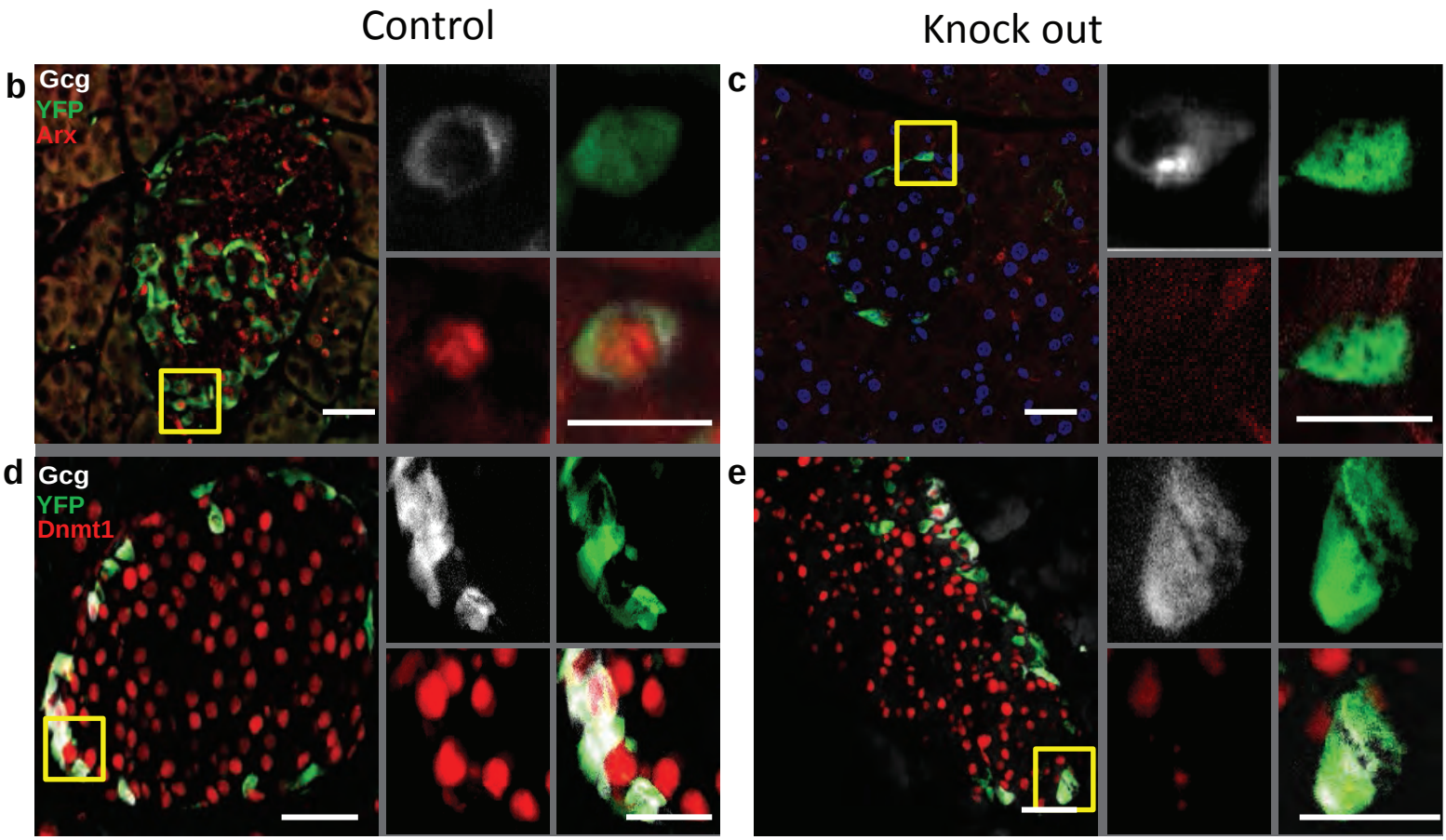

**Figure S2, Related to Figure 1: Cells undergoing α-to-β-cell conversion 4 weeks after deletion of Arx**

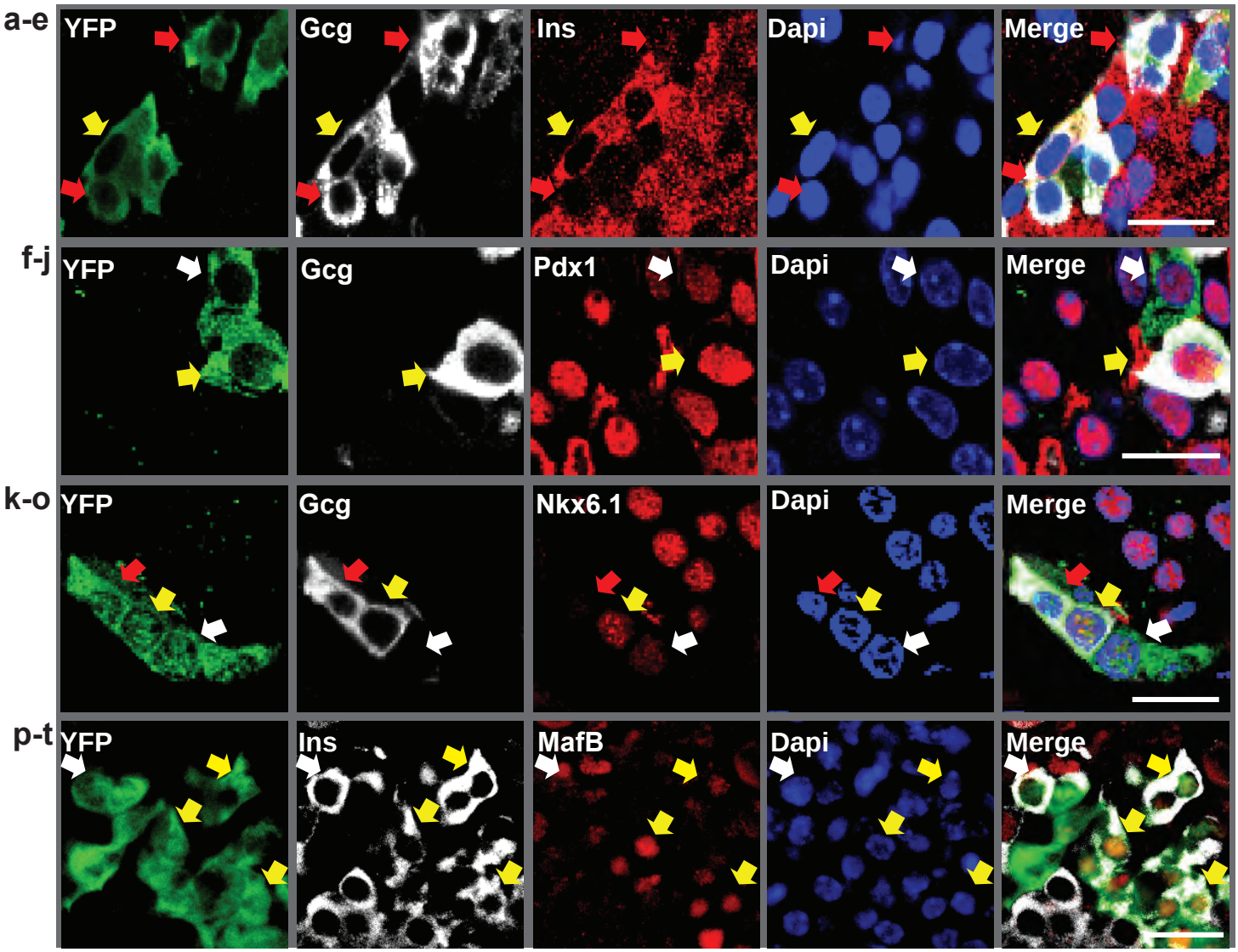

**Supplemental Figure 3, Related to Figure 1: Expression of other islet hormones in α-cells lacking Arx**

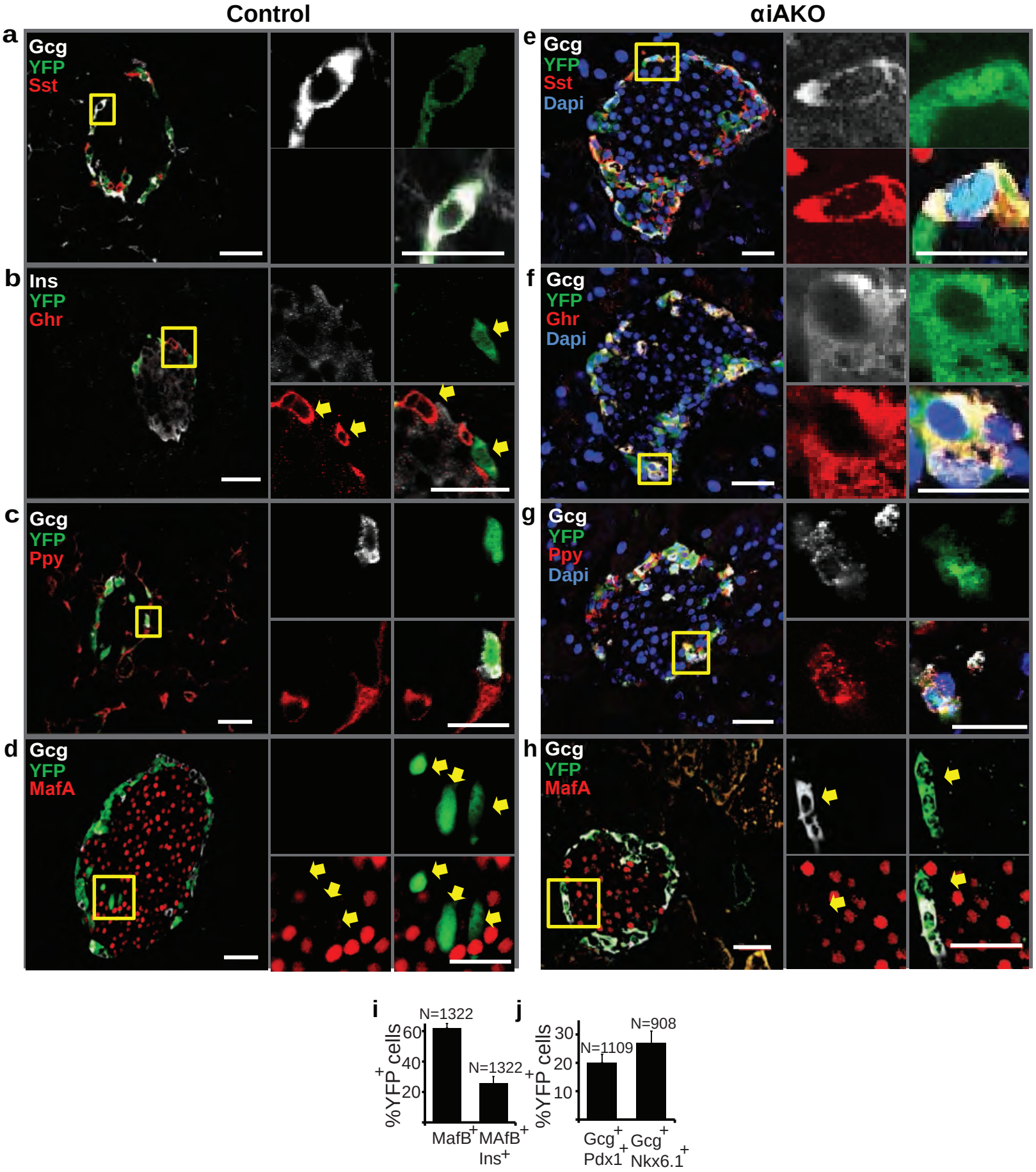

**Figure S4, Related to Figure 3: Cells undergoing α-to-β-cell conversion 4 weeks after deletion of Dnmt1 and Arx**

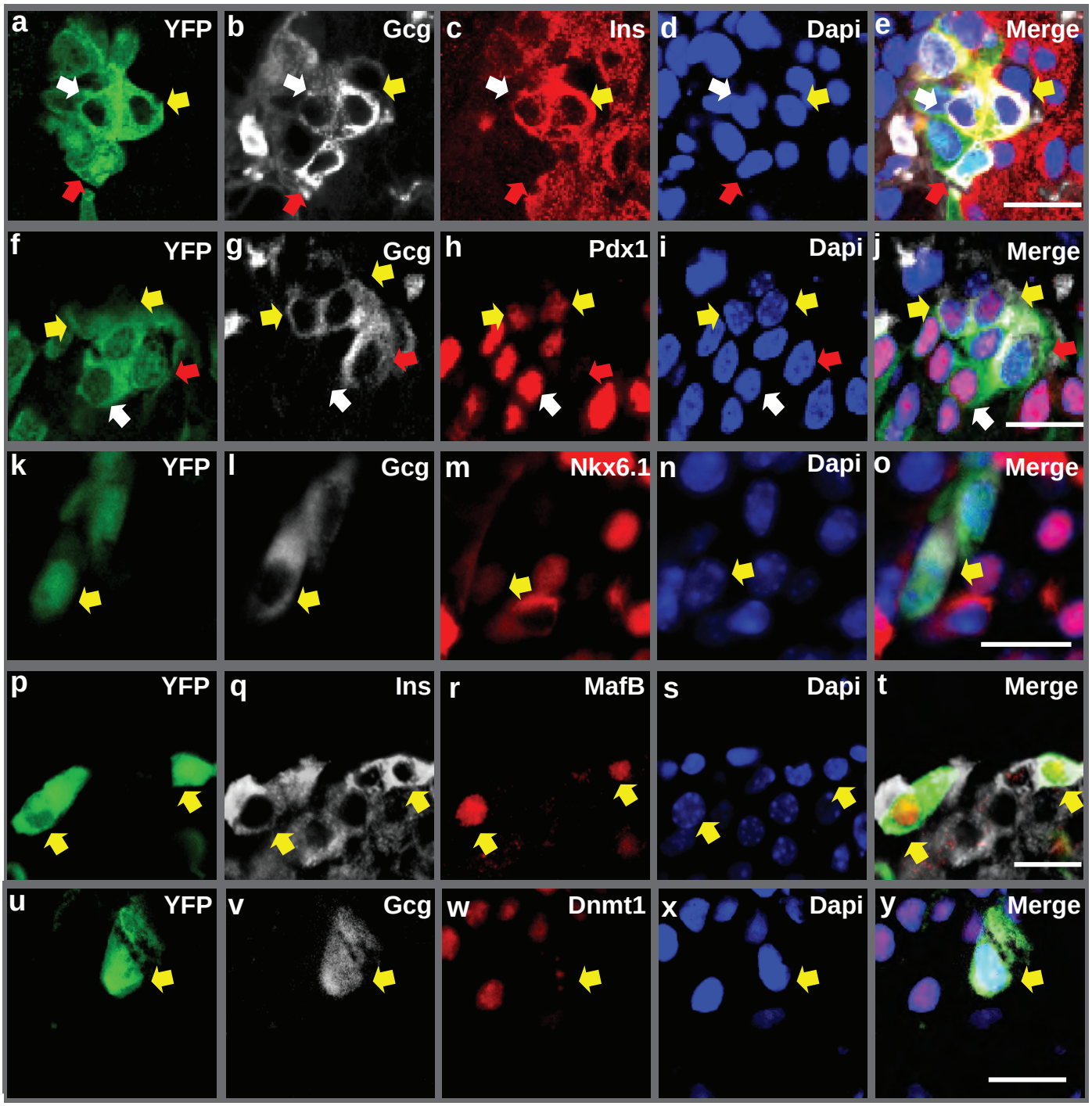


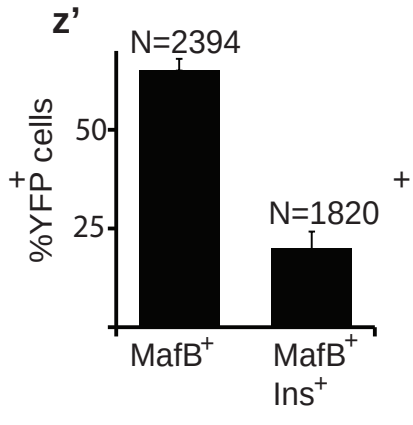


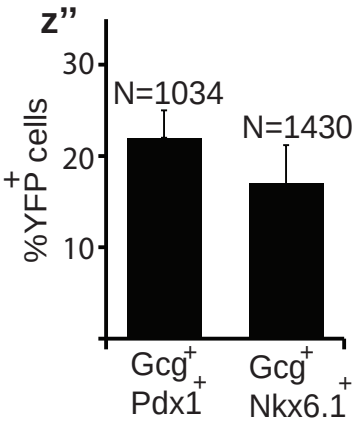


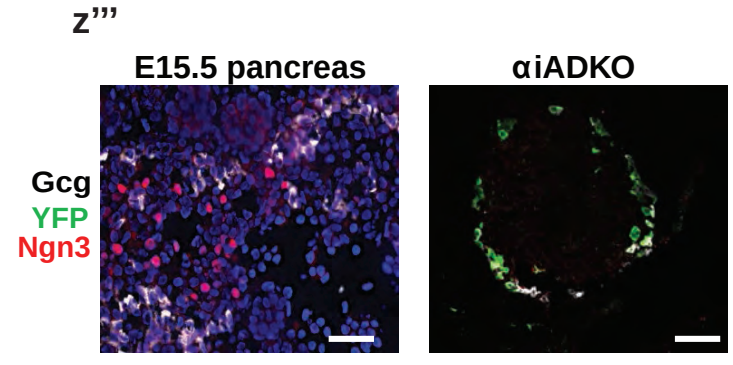

**Supplemental Figure 5 (Related to Figure 6): Glucagon secretion in native α-cells, native β-cells and unconverted α-cells**

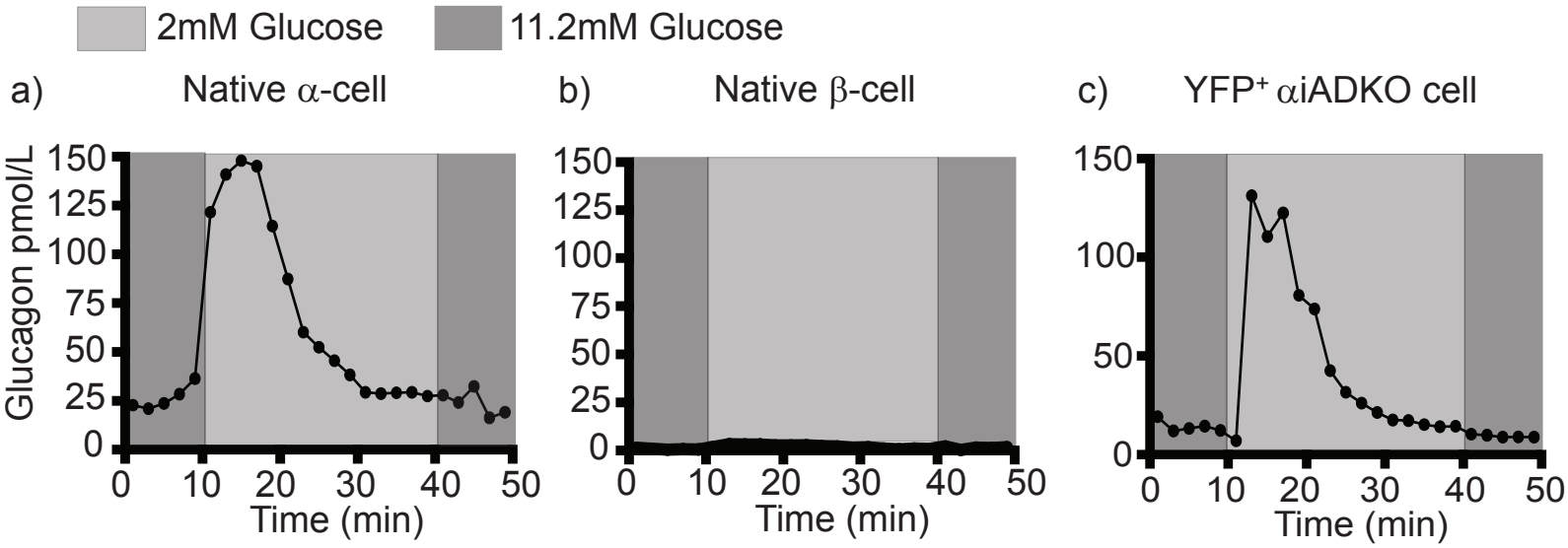

**Supplementary Figure 6, Related to Table 1 and Supplementary Figure 7: Loss of islet cell identity in type 1 diabetes**

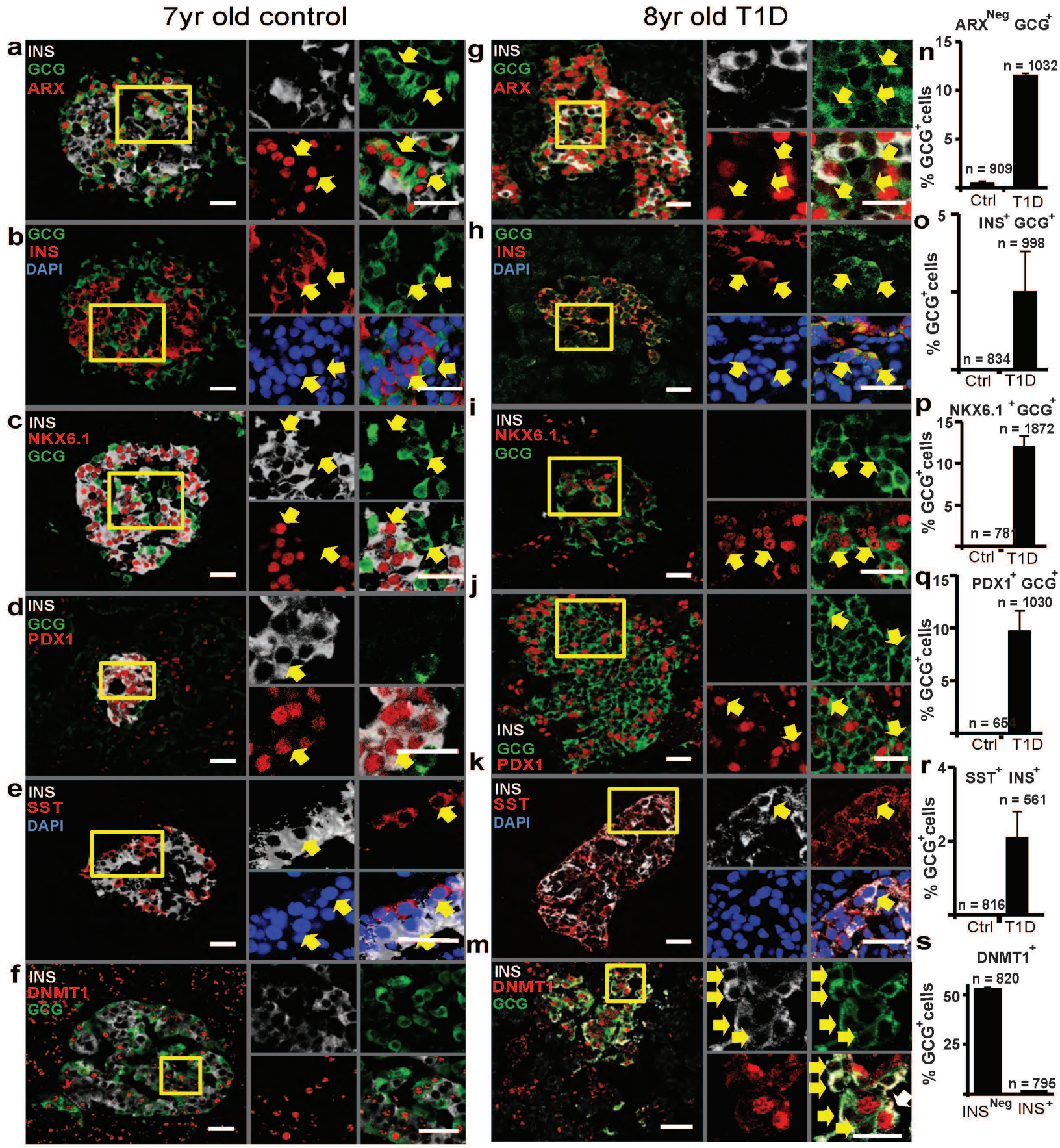

**Supplemental Figure 7, Related to Table 1 and Supplemental Figure 6: Loss of Islet cell identity in type 1 diabetes**

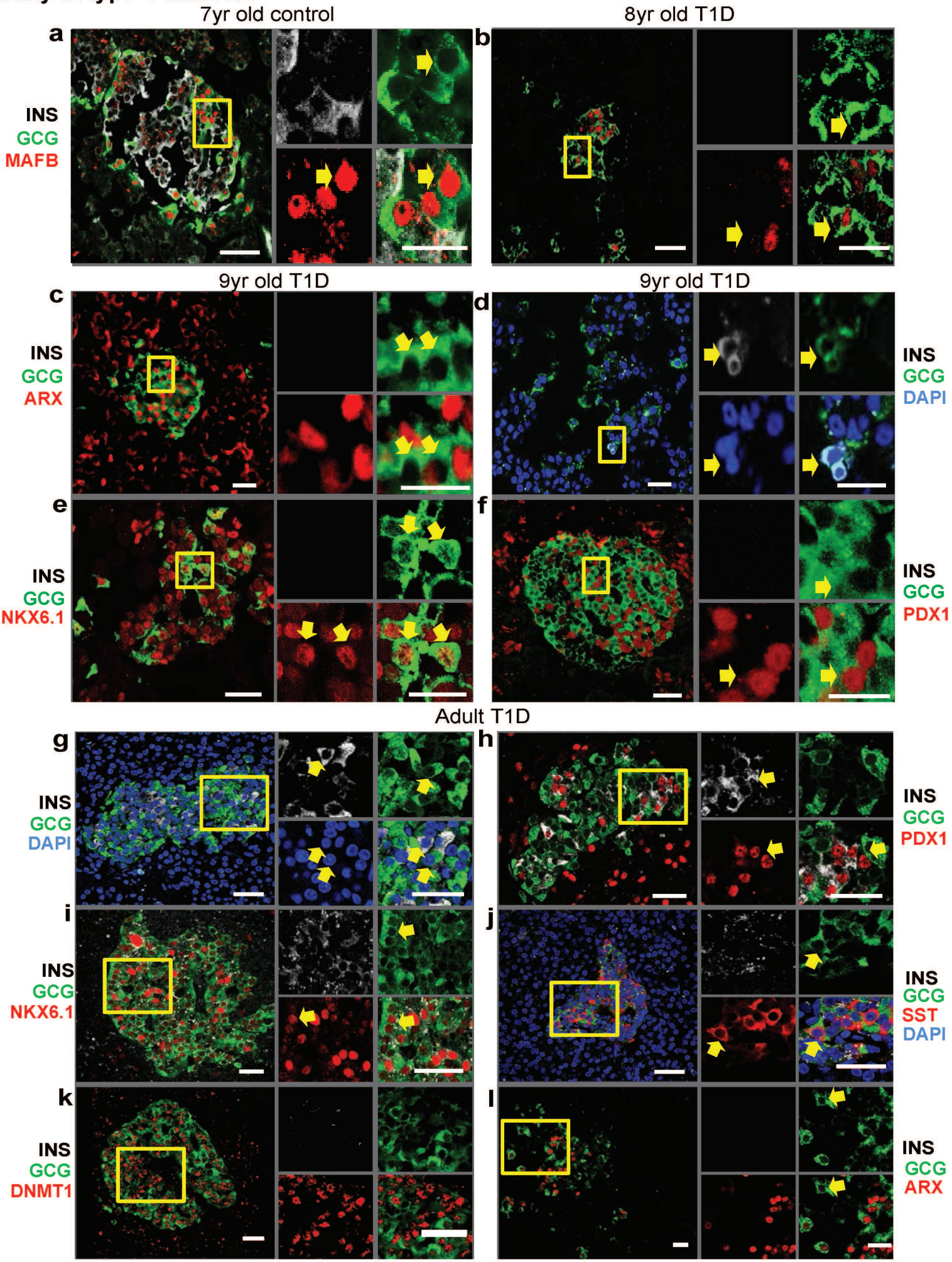

**Supplemental Figure 1, Related to Figures 1-3: Experimental Strategy and Immunostaining demonstrating loss of Arx and Dnmt1 in knock-out mice.**

(a) Schematic showing Doxycycline inducible α-cell knock out mouse generation strategy.

(b,c) Immunostaining showing expression of Arx, YFP and Gcg in control and αiADKO pancreas samples. 979 $YFP^+$ cells were scored in the mutant mice, out of which 930 cells were $Arx^{Neg}$ (95%). 455 $YFP^+$ cells were scored in control mice out of which 450 cells were $Arx^+$ (99%) .

(d,e) Immunostaining showing expression of Dnmt1, YFP and Gcg in control and αiADKO pancreas samples. 1022 $YFP^+$ cells were scored in the mutant mice, out of which 920 cells were $Dnmt1^{Neg}$ (90%). 504 $YFP^+$ cells were scored in control mice out of which 487 cells were $Dnmt1^+$ (96%). Yellow boxes show specific area of islet enlarged and represented on the right to demonstrate gene expression within specific cells or sets of cells. Scale bars represent 25 μm.

**Supplemental Figure 2, Related to Figure 1: Cells undergoing α-to-β-cell conversion 4 weeks after deletion of Arx.**

(a-e) Immunostaining showing coexpression of YFP, Gcg and Ins within a cell (yellow arrow), and coexpression of YFP and Gcg alone within the same cells (red arrows).

(f-j) Immunostaining showing coexpression of YFP, Gcg and Pdx1 within a cell (yellow arrow), and coexpression of YFP and Pdx1 alone within a cell (white arrow).

(k-o) Immunostaining showing coexpression of YFP, Gcg and Nkx6.1 within a cell (yellow arrow), coexpression of YFP and Gcg alone within a cell (red arrow), and coexpression of YFP and Nkx6.1 alone within a cell (white arrow).

(p-t) Immunostaining showing coexpression of YFP, Ins and MafB within a cell, and coexpression of YFP and Ins alone within a cell. Scale bars represent 25 µm.

**Supplemental Figure 3, Related to Figure 1, 2 and 3: Expression of other islet hormones in α-cells lacking Arx**.

(a-c, e-g) Immunostaining showing expression of Sst, Ghrelin and PPY in control (a-c) and αiAKO (e-g) samples.

(d,h) Immunostaining showing expression of MafA in control and αiAKO samples. Yellow boxes show specific area of islet enlarged and represented on the right to demonstrate gene expression within specific cells or sets of cells. Scale bars represent 25 µm.

(i) Percentage of $YFP^+$ cells that express MafB or MafB and Insulin in αiAKO mice 4 weeks after Dox treatment. N represents the total number of cells scored.

(j) Percentage of $YFP^+$ cells that coexpress Gcg and Pdx1 or Gcg and Nkx6.1 in αiAKO mice 4 weeks after Dox treatment. N represents the total number of cells scored.

**Supplemental Figure 4, Related to Figure 3: Cells undergoing α-to-β-cell conversion 4 weeks after deletion of Dnmt1 and Arx.**

(a-e) Immunostaining showing coexpression of YFP, Gcg and Ins within a cell (yellow arrow), coexpression of YFP and Gcg alone within a cell (red arrows), and coexpression of YFP and Ins alone within a cell (white arrow).

(f-j) Immunostaining showing coexpression of YFP, Gcg and Pdx1 within the same cells (yellow arrows), and coexpression of YFP and Pdx1 alone within a cell (white arrow).

(k-o) Immunostaining showing coexpression of YFP, Gcg and Nkx6.1 within a cell (yellow arrow).

(p-t) Immunostaining showing coexpression of YFP, Ins and MafB within the same cells.

(u-y) Immunostaining showing loss of Dnmt1 in a $YFP^+$ $Gcg^+$ cell (u-y). Scale bars represent 25 μm.

(z', z'', z''') Quantification of α and β-cell genes in murine α-cells lacking Dnmt1 and Arx . Percentage of $YFP^+$ cells that express MafB or MafB and Insulin in αiADKO mice 4 weeks after Dox treatment. N represents the total number of cells scored (z'). Percentage of $YFP^+$ cells that coexpress Gcg and Pdx1 or Gcg and Nkx6.1 in αiADKO mice 4 weeks after Dox treatment. N represents the total number of cells scored (z''). Immunostaining showing Neurogenin 3 staining in e15.5 pancreas and αiADKO pancreas (z'''). Scale bars represent 25 μm.

**Supplemental Figure 5 Related to Figure 6: Glucagon secretion in native α-cells, native β-cells and unconverted α-cells.**

(a-c) Temporal glucagon secretion profiles of 5000 $YFP^+$ cells from Glucagon-Venus mice (N=3 mice) (a), MIP-GFP mice (N=3 mice) (b) and αiADKO mice (N=4 mice) (c) perfused with 11.2mM Glucose and 2mM Glucose at the indicated time-points.

**Supplemental Figure 6, Related to Table 1 and Figure S7: Loss of islet cell identity in type 1 diabetes**.

(a-m) Immunostaining showing expression of ARX, NKX6.1, PDX1, Somatostatin (SST), DNMT1, Insulin (INS) and Glucagon (GCG) in control 7 year old pancreatic islets (a-f) and 8yr old T1D islets (g-m). Yellow boxes show specific area of islet enlarged and yellow arrows mark

cells losing α-cell markers or gaining β-cell markers. White arrow (m) marks a rare bi-hormonal $GCG^+$ $INS^+$ cell with detectable nuclear DNMT1. Scale bars represent 25 µm. Quantification of abnormal $GCG^+$ cells in type 1 diabetic and control samples is represented as a percentage of total $GCG^+$ cells counted per sample. N refers to the total number of cells scored in control and type 1 diabetic samples. Bar graph data are represented as mean ± S.D. (n-s).

**Supplemental Fig. 7: Loss of islet cell identity in adult type 1 diabetic samples.**

(a, b) Immunostaining showing expression of MAFB, INS and GCG in control 7 year old pancreatic islets (a) and 8 year old T1D islets (b).

(c-f) Immunostaining showing ARX, NKX6.1, PDX1, INS and GCG in 9 yr old T1D islets.

(g-l) Immunostaining showing expression of PDX1, NKX6.1, SST, DNMT1, ARX, INS and GCG in 32 year old T1D pancreas sample obtained from nPOD (See Table 1). Yellow boxes show specific area of islet enlarged and represented by arrows on the right to demonstrate gene expression within specific cells or sets of cells. Scale bars represent 25 µm. Quantification of abnormal $GCG^+$ cells in the nPOD samples was performed as described in Methods. 5% of $GCG^+$ cells were $ARX^{Neg}$, 5.2% were $NKX6.1^+$, 1% were $SST^+$, 3.4% were $DNMT1^{Neg}$, and 0% were $PDX1^+$ or $INS^+$.

**Supplemental Table 1, Related to Figure 1: Quantification of immunostaining in αiAKO and control mice**

a) αiAKO

| Immunostaining | # islets scored per mouse | Total # YFP$^+$ cells scored |
|---|---|---|
| YFP, Ins, MafB | Mouse 1: 30<br>Mouse 2: 34<br>Mouse 3: 27<br>Mouse 4: 31 | 3245 |
| YFP, Ins, Gcg | Mouse 1: 32<br>Mouse 2: 33<br>Mouse 3: 39<br>Mouse 4: 40 | 3298 |
| YFP, Nkx6.1, Gcg | Mouse 1: 31<br>Mouse 2: 30<br>Mouse 3: 35<br>Mouse 4: 38 | 3457 |
| YFP, Gcg, Pdx1 | Mouse 1: 34<br>Mouse 2: 29<br>Mouse 3: 36<br>Mouse 4: 33 | 3423 |
| YFP, Gcg, MafA | Mouse 1: 35<br>Mouse 2: 30<br>Mouse 3: 32<br>Mouse 4: 28 | 2358 |
| YFP, Ins, Ghr | Mouse 1: 30<br>Mouse 2: 22<br>Mouse 3: 40<br>Mouse 4: 31 | 3021 |
| YFP, Gcg, PPY | Mouse 1: 32<br>Mouse 2: 33<br>Mouse 3: 39<br>Mouse 4: 40 | 2698 |
| YFP, Sst, Gcg | Mouse 1: 29<br>Mouse 2: 34<br>Mouse 3: 39<br>Mouse 4: 34 | 3124 |
| YFP, Neurog3, Gcg | Mouse 1: 32<br>Mouse 2: 33<br>Mouse 3: 39<br>Mouse 4: 40 | 2588 |

b) Control

| Immunostaining | # islets scored per mouse | Total # YFP$^+$ cells scored |
|---|---|---|
| YFP, Ins, MafB | Mouse 1: 28<br>Mouse 2: 27<br>Mouse 3: 30<br>Mouse 4: 34 | 2989 |
| YFP, Ins, Gcg | Mouse 1: 32<br>Mouse 2: 32<br>Mouse 3: 38<br>Mouse 4: 39 | 3240 |
| YFP, Nkx6.1, Gcg | Mouse 1: 29<br>Mouse 2: 25<br>Mouse 3: 30<br>Mouse 4: 37 | 3145 |
| YFP, Gcg, Pdx1 | Mouse 1: 29<br>Mouse 2: 35<br>Mouse 3: 31<br>Mouse 4: 34 | 3342 |
| YFP, Gcg, MafA | Mouse 1: 31<br>Mouse 2: 32<br>Mouse 3: 32<br>Mouse 4: 25 | 2014 |
| YFP, Ins, Ghr | Mouse 1: 31<br>Mouse 2: 34<br>Mouse 3: 23<br>Mouse 4: 27 | 2891 |
| YFP, Gcg, PPY | Mouse 1: 31<br>Mouse 2: 32<br>Mouse 3: 41<br>Mouse 4: 34 | 2349 |
| YFP, Sst, Gcg | Mouse 1: 24<br>Mouse 2: 31<br>Mouse 3: 38<br>Mouse 4: 31 | 2990 |
| YFP, Neurog3, Gcg | Mouse 1: 31<br>Mouse 2: 31<br>Mouse 3: 35<br>Mouse 4: 24 | 2331 |

**Supplemental Table 2, Related to Figures 2 and 3: Quantification of immunostaining in αiDKO and αiADKO**

a) αiDKO mice

| Immunostaining | # islets scored per mouse | Total # YFP$^+$ cells scored |
|---|---|---|
| YFP, Gcg, MafB | Mouse 1: 23<br>Mouse 2: 27<br>Mouse 3: 21<br>Mouse 4: 28 | 2091 |
| YFP, Ins, Pdx1 | Mouse 1: 26<br>Mouse 2: 26<br>Mouse 3: 21<br>Mouse 4: 24 | 2011 |
| YFP, Ghr, Pdx1 | Mouse 1: 23<br>Mouse 2: 25<br>Mouse 3: 26<br>Mouse 4: 20 | 1990 |
| YFP, Ins, Nkx6.1 | Mouse 1: 23<br>Mouse 2: 21<br>Mouse 3: 25<br>Mouse 4: 24 | 1945 |
| YFP, Ins, Gcg | Mouse 1: 22<br>Mouse 2: 25<br>Mouse 3: 24<br>Mouse 4: 21 | 2003 |

b) αiADKO

| Immunostaining | # islets scored per mouse | Total # YFP$^+$ cells scored |
|---|---|---|
| YFP, Ins, Gcg | Mouse 1: 27<br>Mouse 2: 30<br>Mouse 3: 35<br>Mouse 4: 43 | 3446 |
| YFP, Ins, MafB | Mouse 1: 32<br>Mouse 2: 30<br>Mouse 3: 38<br>Mouse 4: 37 | 3250 |
| YFP, Gcg, MafB | Mouse 1: 23<br>Mouse 2: 25<br>Mouse 3: 30<br>Mouse 4: 28 | 2190 |
| YFP, Gcg, Pdx1 | Mouse 1: 30<br>Mouse 2: 32<br>Mouse 3: 39<br>Mouse 4: 39 | 3560 |
| YFP, Nkx6.1, Gcg | Mouse 1: 34<br>Mouse 2: 36<br>Mouse 3: 35<br>Mouse 4: 30 | 3430 |
| YFP, Nkx6.1, Ins | Mouse 1: 33<br>Mouse 2: 23<br>Mouse 3: 26<br>Mouse 4: 29 | 2887 |
| YFP, Slc2a2, Gcg | Mouse 1: 24<br>Mouse 2: 26<br>Mouse 3: 29<br>Mouse 4: 20 | 2309 |
| YFP, Gcg, MafA | Mouse 1: 34<br>Mouse 2: 34<br>Mouse 3: 38<br>Mouse 4: 35 | 3320 |
| YFP, Ins, Ghr | Mouse 1: 24<br>Mouse 2: 30<br>Mouse 3: 21<br>Mouse 4: 26 | 2339 |
| YFP, Gcg, PPY | Mouse 1: 23<br>Mouse 2: 25<br>Mouse 3: 29<br>Mouse 4: 24 | 2431 |
| YFP, Sst, Gcg | Mouse 1: 30<br>Mouse 2: 21<br>Mouse 3: 23<br>Mouse 4: 24 | 2341 |
| YFP, Neurog3, Gcg | Mouse 1: 32<br>Mouse 2: 33<br>Mouse 3: 31<br>Mouse 4: 29 | 3039 |

## Supplemental Table 3, Related to Figure 1 and 3: Details of quantification of Ki67 immunostaining

**a) Ki67 immunostaining in αiAKO mice (4 wk time-point)**

| Mouse | # islets scored | Total $Gcg^+$ cells scored | Total $Ki67^+$ $Gcg^+$ cells scored |
|---|---|---|---|
| Mouse 1 | 25 | 297 | 2 |
| Mouse 2 | 31 | 320 | 2 |
| Mouse 3 | 24 | 311 | 1 |

**b) Ki67 immunostaining in αiAKO mice (4 wk time-point)**

| Mouse | # islets scored | Total $Gcg^+$ cells scored | Total $Ki67^+$ $Gcg^+$ cells scored |
|---|---|---|---|
| Mouse 1 | 26 | 300 | 2 |
| Mouse 2 | 28 | 299 | 3 |
| Mouse 3 | 32 | 319 | 3 |

**c) Ki67 immunostaining in αiADKO mice (4 wk time-point)**

| Mouse | # islets scored | Total $Gcg^+$ cells scored | Total $Ki67^+$ $Gcg^+$ cells scored |
|---|---|---|---|
| Mouse 1 | 25 | 389 | 2 |
| Mouse 2 | 28 | 401 | 0 |
| Mouse 3 | 27 | 416 | 1 |

**d) Ki67 immunostaining in αiADKO mice (12 wk time-point)**

| Mouse | # islets scored | Total $Gcg^+$ cells scored | Total $Ki67^+$ $Gcg^+$ cells scored |
|---|---|---|---|
| Mouse 1 | 21 | 354 | 2 |
| Mouse 2 | 25 | 398 | 3 |
| Mouse 3 | 22 | 403 | 2 |

**Supplementary Table 4, Related to Figures 1, 2 and 3: Details of glycemia in control and knock out mice during ad libitum feeding and fasting.**

**a) Glycemia in fasted or ad libitum fed control mice (4 wk time-point)**

| Mouse | Fasting glucose (mg//dL) | Ad libitum fed glucose (mg/dL) |
|---|---|---|
| Mouse 1 | 74 | 198 |
| Mouse 2 | 60 | 143 |
| Mouse 3 | 93 | 100 |
| Mouse 4 | 79 | 124 |
| Average | 76.5 | 141.25 |

**b) Glycemia in fasted or ad libitum fed αiAKO mice (4 wk time-point)**

| Mouse | Fasting glucose (mg//dL) | Ad libitum fed glucose (mg/dL) |
|---|---|---|
| Mouse 1 | 53 | 200 |
| Mouse 2 | 70 | 155 |
| Mouse 3 | 110 | 130 |
| Mouse 4 | 85 | 188 |
| Average | 79.5 | 168.25 |

**c) Glycemia in fasted or ad libitum fed αiADKO mice (4 wk time-point)**

| Mouse | Fasting glucose (mg//dL) | Ad libitum fed glucose (mg/dL) |
|---|---|---|
| Mouse 1 | 66 | 213 |
| Mouse 2 | 98 | 200 |
| Mouse 3 | 90 | 167 |
| Mouse 4 | 67 | 100 |
| Average | 80.25 | 170 |

**d) Glycemia in fasted or ad libitum fed αiDKO mice (4 wk time-point)**

| Mouse | Fasting glucose (mg//dL) | Ad libitum fed glucose (mg/dL) |
|---|---|---|
| Mouse 1 | 87 | 245 |
| Mouse 2 | 85 | 168 |
| Mouse 3 | 54 | 140 |
| Mouse 4 | 120 | 178 |
| Average | 86.5 | 182.75 |

**No significant differences in fasting or ad libitum fed glucose levels between control and knock out mice**

**Supplementary Table 5, Related to Figures 1-3, S1-4, S6-7: List of primary antibodies**

| Antibody | Source | Dilution | Antigen Retrieval | Amplification |
|---|---|---|---|---|
| Guinea pig anti-Insulin | Dako A0564 | 1:500 | No | No |
| Mouse anti-Insulin | Sigma Aldrich I2018 clone K36AC10 | 1:500 | No | No |
| Rabbit anti-C-peptide | Cell Signaling Technology 4593b | 1:500 | No | No |
| Guinea pig anti-Glucagon | Linco 4031-01 | 1:500 | No | No |
| Mouse anti-Glucagon | Sigma Aldrich G2654 clone K79bB10 | 1:500 | No | No |
| Rabbit anti-Glucagon | Dako A0565 | 1:500 | No | No |
| Goat anti-Arx | Santa Cruz Biotechnology sc-48843 | 1:200 | Yes | Yes |
| Sheep anti-Arx | R&D Systems AF7068 | 1:1500 | Yes | Yes |
| Mouse anti-Nkx6.1 | DSHB F55A10 | 1:200 | Yes | Yes |
| Rabbit anti-Nkx6.1 | Novo Nordisk Antibody core | 1:200 | Yes | Yes |
| Goat anti-Pdx1 | Santa Cruz Biotechnology sc-14664 | 1:200 | Yes | Yes |
| Goat anti-Somatostatin | Santa Cruz Biotechnology sc-7819 lot J0907 | 1:200 | No | No |
| Rabbit anti-Somatostatin | Dako A056601-2 | 1:200 | No | No |
| Mouse anti-Dnmt1 | Abcam ab92453 | 1:500 | Yes | Yes |
| Rabbit anti-MafB | Bethyl laboratories IHC-00351 lot 1 | 1:200 | Yes | Yes |
| Rabbit anti-Chromogranin A | Immunostar, Hudson, WI 20085 | 1:200 | No | No |
| Mouse anti-Chromogranin A | Cell Marque, Rocklin, CA LK2H10 | 1:200 | No | No |
| Mouse anti-Nkx2.2 | DSHB 74.5A5 | 1:50 | Yes | Yes |
| Mouse anti-Pax6 | DSHB | 1:200 | Yes | Yes |
| Chicken anti-YFP | Abcam ab13970 | 1:200 | No | No |
| Mouse anti-Neurog3 | DSHB F25A1B3 | 1:500 | Yes | No |
| Rabbit anti-Ki67 | Leica Microsystems, Germany NCL-Ki67p | 1:100 | Yes | No |
| Goat anti-PPY | Novus Biologicals, Littleton, CO NB100-1793 lot P1 | 1:200 | No | No |
| Goat anti-Ghrelin | Santa Cruz Biotechnology sc-10368 | 1:200 | No | No |
| Goat anti-Glut2 | Santa Cruz Biotechnology sc-7580 | 1:200 | No | No |

**Supplementary Table 6, Related to Figures 1-3, S1-4, S6-7: List of secondary antibodies**

| Antibody | Dilution | Wavelength | Catalog # |
|---|---|---|---|
| Goat anti-Chicken | 1:200 | Alexa Fluor 488 | A-11039 |
| Goat anti-Mouse | 1:200 | Alexa Fluor 488 | A-11029 |
| Goat anti-Rabbit | 1:200 | Alexa Fluor 488 | A-11008 |
| Goat anti-Mouse | 1:200 | Alexa Fluor 555 | A-21425 |
| Goat anti-Rabbit | 1:200 | Alexa Fluor 555 | A-21428 |
| Goat anti-Guinea pig | 1:200 | Alexa Fluor 647 | A-21450 |
| Goat anti-Mouse | 1:200 | Alexa Fluor 647 | A-21235 |
| Donkey anti-Goat | 1:200 | Alexa Fluor 555 | A-21432 |

Supplemental Methods

**Human Tissues** Institutional review board approval for research use of human tissue was obtained from the Stanford University School of Medicine. Pancreas specimens were obtained from the International Institute for the advancement of Medicine (IIAM) and the network of pancreatic organ donors (nPOD) (Table 1). De-identified normal human pancreas specimens from donors aged 4, 7, and 26 years, and 2 pancreas specimens from type 1 diabetic donors with short disease duration aged 8 and 9 years were obtained from IIAM and fixed in 4% paraformaldehyde, then embedded in OCT before subsequent sectioning (9 µm). Pancreas specimens from three type 1 diabetic donors with long-standing disease were obtained as slides from nPOD (Table 1).

**Mouse studies** All animal experiments and methods were approved by the Institutional Animal Care and Use Committee (IACUC) of Stanford University. *Glucagon-rtTA, Tet-o-Cre, R26-YFP*, mice have been described previously (Thorel et al., 2010). The *Dnmt1*$^{f/f}$ mice were a gift from Dr. L. Jackson-Grusby (Jackson-Grusby et al., 2001). The *Arx*$^{f/f}$ mice were a gift from Dr. J. Golden (Fulp et al., 2008).

**Immunohistology and Confocal Microscopy** Human pancreas sections were stained with antibodies against a panel of endocrine genes listed in Table S5a as described previously (Chen et al., 2011). In brief, slides were washed with PBS, blocked with normal donkey serum (5%) and primary antibodies were applied. Antigen retrieval was performed by boiling the slides in Antigen retrieval solution (S1699; DAKO; Carpinteria, CA) for 10 minutes before blocking. The Neurog3, Nkx2.2, Nkx6.1, Pdx1 and Pax6 antibodies were developed by Dr OD Madsen and obtained from the Developmental Studies Hybridoma Bank (DSHB) developed under the auspices of the NICHD and maintained by the University of Iowa, Department of Biological

Sciences, Iowa City, IA 52242. Stained sections were mounted with VECTASHIELD Mounting Medium with Dapi (H-1200, Vector Laboratories). Staining was visualized using a Leica SP2 inverted confocal laser scanning microscope at a magnification of 63X (oil immersion) with Ar/Kr, He/Ne and 405 nm lasers. Each image was scanned as a Z-stack with a total thickness of 1.5-2 µm and 10 optical slices of equal thickness (0.15-0.2 µm). Each color was scanned independently.

**Flow Cytometry** Isolated mouse islets were dissociated into single cells by enzymatic digestion using 0.05% Trypsin (25300-120; Life Technologies). 7-aminoactinomycin D (7-AAD, eBiosciences) was used at 1:500 dilution as Live/Dead stain to exclude dead cells. Sort gates were adjusted with reference to negative controls (wild-type islets without YFP labeling). Cells were sorted on a special order 5-laser FACS Aria II (BD Biosciences) using a 100 µm nozzle at a flow rate of 1 following doublet removal. Sorted single-cells were collected directly into 96-well plates (Bio-Rad cat #: HSP9601) containing 4 µL of lysis buffer with dNTPs[37] for downstream single-cell RNA-Seq assays.

**Single-Cell RNA-Seq and Data Analysis** Single-cell RNA-Seq libraries were generated as described (Picelli et al., 2014). Briefly, single-cells collected in 96-well plates were lysed, followed by reverse transcription with template-switch using an LNA-modified template switch oligo to generate cDNA. After 21 cycles of pre-amplification, DNA was purified and analyzed on an automated Fragment Analyzer (Advanced Analytical). Each cell's cDNA fragment profile was individually inspected and only wells with successful amplification products (concentration higher than 0.06 ng/ul) and with no detectable RNA degradation were selected for final library

preparation. Tagmentation assays and barcoded sequencing libraries were prepared using Nextera XT kit (FC-131-1024; Illumina) according to the manufacturer's instructions. Barcoded libraries were pooled and subjected to 75 bp paired-end sequencing on the Illumina NextSeq instrument. Sequencing reads were trimmed, adapter sequences removed and the reads aligned using STAR (Dobin et al., 2015) with default parameters. Duplicate reads were removed using picard (McKenna et al., 2010). Transcript counts were obtained using HT-Seq (Anders et al., 2015) and mm10 UCSC exon/transcript annotations. Pairwise distances between cells were estimated using Pearson correlation of overdispersed genes as described (Fan et al., 2016). Subsequent hierarchical clustering was done using hclustfunction in R, and dimension reduction was performed using the *t*-SNE method on pairwise distances (Van der Maaten and Hinton, 2008). Data were also analyzed with QIAGEN Ingenuity® Pathway Analysis (IPA®, QIAGEN Redwood City, www.qiagen.com/ingenuity) with the following analysis settings: Expression Value Type (Exp Log Ration), Range (-4.78 to 4.93; 80 analysis molecules across observations), Reference set (Ingenuity Knowledge Base + Endogenous chemicals), Relationships to consider (Direct and Indirect Relationships), Interaction networks (35 molecules/network; 25 networks/analysis), Data Source (All), Confidence (Experimentally Observed), Species (All), Tissue & Cell Lines (none), Mutations (All). The GEO accession number is GSE79457.

**Electrophysiological studies**

Islets from control or αiADKO mice were dispersed to single cells and plated overnight on 35-mm dishes as previously (Dai et al., 2011). Cells were patch-clamped in the whole-cell voltage-clamp configuration in a heated bath at 32-35ºC using a HEKA EPC10 amplifier and PatchMaster Software (Heka Electronik, Germany) and patch pipettes with resistances of 4 ~ 5 MΩ after fire polishing. $Na^+$ channels were activated by a depolarization to 0 mV following

holding potentials ranging from -140 to 0 mV. For this, the bath solution contained (in mM): 118 NaCl, 5.6 KCl, 1 $MgCl_2$, 2.6 $CaCl_2$, 20 TEA-Cl, 5 HEPES, 5 glucose, 50 nM ω-conotoxin, and 10 μM isradipine (pH 7.4 with NaOH). The pipette solution for these experiments contained (in mM): 125 Cs-glutamate, 1 $MgCl_2$, 10 EGTA, 1 HEPES, and 3 MgATP (pH 7.15 with CsOH). Single cell exocytosis was measured essentially as described previously (Ferdaoussi et al., 2015). Briefly, cells were pre-incubated at either 2 or 20 mM glucose for 1 hour and transferred to bath solution with either 20 or 2 mM glucose ~10-30 minutes prior to patch-clamping. Exocytosis was elicited by a series of ten 500-ms membrane depolarizations from -70 to 0 mV and monitored as increases in cell capacitance. For this, the bath solution was (in mM): 118 NaCl, 20 TEA, 5.6 KCl, 1.2 $MgCl_2$, 2.6 $CaCl_2$, 5 HEPES, and either 20 or 2 glucose (pH 7.4 with NaOH). The pipette solution contained (in mM): 125 Cs-glutamate, 10 CsCl, 10 NaCl, 1 $MgCl_2$, 0.05 EGTA, 5 HEPES, 0.1 cAMP and 3 MgATP (pH 7.15 with CsOH). Following the experiments cells were immunostained for insulin (polyclonal guinea pig anti-insulin from Dako, detected by goat anti-guinea pig Alexa Fluor 594 secondary from Invitrogen) and YFP (rabbit anti-GFP primary and AlexaFluor 488 anti-rabbit secondary, Invitrogen) to identify β-cells ($Ins^+$ only), α-cells ($YFP^+$ only) or converted α-cells ($Ins^+$,$YFP^+$). Data were analyzed using FitMaster (Heka Electronik) and Prism v6.0h (Graphpad Software Inc.). Statistical analysis of exocytosis data was by 2-way ANOVA followed by Bonferroni post-test ($P$<0.05 considered significant).

**Hormone secretion and Calcium Imaging**

Hormone secretion and calcium imaging studies were performed as previously described (Adewola et al., 2010; Xing et al., 2016). Briefly, islets from MIP-GFP, Glucagon-Venus, and αiADKO mice were dispersed into single cells and $GFP^+$, $Venus^+$ or $YFP^+$ cells were collected by FACS (MoFlo, Beckman Coulter, CA) as described above.

For calcium imaging, the sorted cells were incubated in Kreb's Ringer Buffer (KRB) with 2mM glucose and 5μM Fura-2/AM (Molecular Probes, CA) for 30 minutes. Cells were then loaded into a temperature equilibrated microfluidic device mounted on an inverted epifluorescence microscope (Leica DMI 4000B). KRB with 14 mM glucose or 2mM glucose with 30mM KCl was administered to the cells for 20 minutes and 15 minutes respectively. Dual-wavelength Fura-2/AM was excited at 340 and 380 nm (shift in excitation wavelength occurs upon binding $Ca^{2+}$), and fluorescent emission was detected at 510 nm. Fura-2 fluorescence emission spectra were filtered using a Fura-2 dichroic beamsplitter and a double band emission filter (Chroma Technology. Part number: 73100bs). The images were collected with a CCD (Retiga-SRV, Fast 1394, QImaging). SimplePCI software (Hamamatsu Corp.) was used for image acquisition and analysis. Intracellular $Ca^{2+}$ concentration was expressed as a ratio of fluorescent emission intensity (% F340/F380). The fluorescence signal was expressed as a change in percentage after being normalized to basal intensity levels established before stimulation.

For hormone secretion studies, 5000 $GFP^+$ cells from MIP-GFP mice, $Venus^+$ cells from Glucagon-Venus mice or $YFP^+$ cells from αiADKO mice were collected by FACS and loaded onto the microfluidic device. To measure insulin secretion, 5000 $YFP^+$ cells were incubated in basal KRB with 2mM glucose for 30 mins and then stimulated with KRB containing 14 mM glucose for 30 mins followed by 2 mM glucose for 10 mins. To measure glucagon secretion, 5000 $YFP^+$ cells were incubated in KRB with 11.2 mM glucose for 30 min and then stimulated with KRB with 2 mM glucose for 30 minutes. For both Insulin and Glucagon measurements, perfusate was collected at a flow rate of 100 μl/minute every 2 minutes. Ultrasensitive Rodent Insulin or Glucagon ELISAs (Mercodia, Uppsala, Sweden) were used to measure perfusate insulin or glucagon levels.